Repurposing Bacterial Extracellular Matrix for Selective and Differential Abstraction of Rare Earth Elements

Journal:	*Green Chemistry*
Manuscript ID	GC-ART-04-2018-001355.R1
Article Type:	Paper
Date Submitted by the Author:	19-Jun-2018
Complete List of Authors:	Tay, Pei Kun; Harvard University, John A. Paulson School of Engineering and Applied Sciences; Harvard University Wyss Institute for Biologically Inspired Engineering Manjula-Basavanna, Avinash; Harvard University, John A. Paulson School of Engineering and Applied Sciences; Harvard University Wyss Institute for Biologically Inspired Engineering Joshi, Neel S.; Harvard University Wyss Institute for Biologically Inspired Engineering

Journal Name

ARTICLE

Repurposing Bacterial Extracellular Matrix for Selective and Differential Abstraction of Rare Earth Elements

Alphagammaco-Full-1400Received 00th January 20xx,
Accepted 00th January 20xx

DOI: 10.1039/x0xx00000x

www.rsc.org/

Pei Kun R. Tay,[a,b] Avinash Manjula-Basavanna[a] and Neel S. Joshi*[a,b]

The rare earth elements (REEs) play critical roles in modern consumer electronics and clean technologies, but unpredictable supply and environmentally unsustainable extraction practices have spurred efforts to develop green methods of recovering the metals from waste streams. In this regard, we have repurposed a bacterial extracellular matrix (ECM) for selective and differential abstraction of REEs. Herein, the curli amyloid fibers in *E. coli* biofilms are genetically modified to display lanthanide binding tags (LBTs). The curli-LBT filters showed lanthanide specificity in the presence of other metals, with a preference for binding several high-value heavy REEs. Bound lanthanides were readily recovered using a dilute acid wash, and the filters could be re-used for multiple cycles of sorption and desorption with minimal loss of efficiency. Our engineered biofilm-derived filters provide a rapid, selective and scalable method for REE separation that is more robust compared to conventional cell-based sorbents, and this platform could be adapted to recover other precious metals or commodities.

Introduction

The rare earth elements (REEs) exhibit unique properties that enable their utilization in modern-day magnets, batteries, phosphors and catalysts.[1] Though not particularly rare in terms of crustal abundance, REEs are found at fairly low concentrations in ores, and are difficult and costly to extract and refine due to their physicochemical similarities.[2,3] Global demand for REEs has grown steadily over the past few decades, a continuing trend driven by their importance to the consumer electronics industry and the clean-energy sector. In recent reports, both the European Union and the United States Department of Energy have identified REEs to be critical to emerging low-carbon energy technologies, yet there are concerns that future REE availability could be compromised by monopolistic supply conditions—China currently controls over 95% of REE supplies—and environmentally unsustainable extraction practices.[1-6] The most widely used separation method is solvent extraction, which requires several steps of pre-treatment with strong acids or bases followed by multiple extraction cycles using organic solvents.[7,8] The solvent waste, if not contained, can create extensive environmental damage leading to the contamination of natural water streams. These detrimental effects, along with the need to establish more reliable supplies of the metals, have led to efforts to recover REEs from waste streams, e.g. mine tailings or consumer product waste.[9,10]

The use of microorganisms for the sustainable removal of toxic metals from industrial waste has been extensively investigated and reviewed.[11] Knowledge of the way some of these metals interact with microorganisms has helped to define remediation strategies, including the design of genetically engineered bacteria and fungi capable of bio-accumulating heavy metals intracellularly, on the cell surface or within an extracellular matrix.[12] Much less is known about the interactions between REEs and microbes. Several lanthanides have recently been discovered to function as cofactors in the alcohol dehydrogenases of bacteria, but it is not clear how the bacteria mobilize or metabolize these metals.[13-15]

Nonetheless, multiple studies in recent years have established that lanthanides passively adsorb to the cell surface of some bacteria and fungi, and that carboxylate- and phosphate-containing entities in the cell wall are the main binding sites for the metals.[16-18] The bound lanthanides could be recovered by treating the cells with competing chelators (e.g. citrate, EDTA) or by washing with an acid, though the latter adversely affected cell viability.[19] The majority of these studies were performed in batch using living cells, which required the growth and maintenance of large volumes of cultures, with the ensuing complication of having to separate the cells from the effluent stream.[19,20] This has partly been resolved by immobilizing the biomass on solid supports like activated alumina, polymer beads and filter membranes. Fixed bed bioreactors assembled from these supports have enabled

[a] Wyss Institute for Biologically Inspired Engineering, Harvard University, Boston, Massachusetts 02115, United States of America.
[b] School of Engineering and Applied Sciences, Harvard University, Cambridge, Massachusetts 02138, United States of America.
Electronic Supplementary Information (ESI) available: [FESEM, time and pH dependent binding of curli-LBTs to REE and other details]. See DOI: 10.1039/x0xx00000x

continuous-flow biosorption and streamlined multiple sorption/desorption cycles.[21] However, the long-term integrity of the immobilized biomass was not studied, and escape of cells or cell debris could potentially occlude flow lines. There have been efforts to reduce the reliance on living cells by using dried cell matter, but this has led to lower binding capacities.[22]

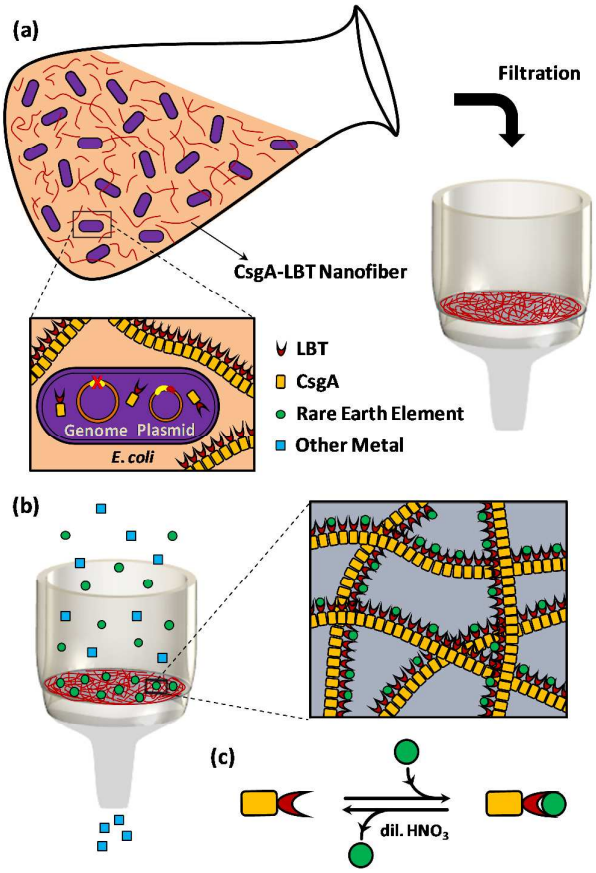

Figure 1. Schematic of extracellular matrix of *E. coli* repurposed for selective (a,b) and reversible (c) binding of rare earth elements (REEs).

Besides the cell surface, extracellular polymers (EPs) secreted by cells in biofilms are also known to bind metals.[23,24] Alginate, an anionic polysaccharide produced by seaweed and some algae, has shown affinity for some lanthanides.[25,26] Wang *et al*. used gel beads comprising a mix of alginate and poly-γ-glutamic acid (an exopolysaccharide produced by *Bacillus* sp.) to recover Nd^{3+} over several sorption/desorption cycles.[27] An issue with alginate-based biosorbents is that the Ca^{2+} commonly used for cross-linking to yield stable gels is prone to be displaced during the binding and desorption phases, thus necessitating frequent replenishment to maintain the structural integrity of the sorbent. It is also difficult to alter the chemical composition of polysaccharides to increase binding affinity or introduce greater REE binding selectivity—a disadvantage in general of relying on non-specific adsorption to cell walls or exopolymers.

Other EPs commonly associated with bacterial biofilms are amyloid fibrils self-assembled from secreted protein monomers. Unlike with sugars, these protein monomers are more tractable to genetic engineering, and our group and others have successfully appended peptide tags and protein domains to one such monomer—the *E. coli* CsgA protein—to create functionalized curli fiber-based biofilms capable of capturing enzymes and metal nanoparticles.[28-34] Further, we have shown that these fibers could be untethered from the cell surface by removing the anchoring protein CsgB, allowing the formation of extensive cell-free fiber meshes (tens of microns in size) that were easily immobilized onto membranes via a filtration process.[35] Here we demonstrate that immobilized curli fiber mats displaying a genetically-encoded lanthanide-binding tag could be used for the binding and release of rare earth metal ions over multiple cycles (Fig. 1).

Lanthanide-binding tags (LBTs) are oligopeptides originally developed as protein tags to study protein structure and interactions *in vitro* and *in vivo*.[36-40] They were evolved to chelate Tb^{3+} over metal ions of similar size (e.g. Ca^{2+}) and valence (e.g. Fe^{3+}), and showed nanomolar binding affinity for many lanthanides.[41] Being small, they could be inserted in loops of proteins or at their termini using standard molecular biology techniques with minimal impact on structure and function.[36,42] Park *et al*. recently appended 8×LBT to the S-layer protein of *Caulobacter crescentus* for cell surface display.[43] The engineered bacteria bound several lanthanides with varying affinities, and the lanthanides were recovered using a citrate treatment. Although the cells were selective for Tb^{3+} over other metals, binding required the presence of Ca^{2+} and relied on batch sorption using living cells, with its attendant disadvantages as described previously. By displaying LBTs on extracellular amyloid fibers that maintain their functionality regardless of the presence of cells, we were able to assemble cell-free materials that retained a large surface area for lanthanide sorption, without the potential for cell contamination in downstream processes. Along similar lines, lactoglobulin amyloid fibrils immobilized on filters have been used to sequester heavy metals.[44] On the other hand, zinc finger inspired lanthanide binding motifs termed lanthanide fingers were shown to bind all lanthanides in a competitive aqueous environment.[45] Crystal structures of native proteins that bind to lanthanide ions show that 69% of the coordination sites are occupied by carboxylate functionalities.[46] By modulating the conformation of the rationally designed protein, reversible binding between Tb^{3+} and Ca^{2+} has also been achieved.[47]

Herein, we show that rare earths could be recovered by repurposing the ECM of *E. coli* through genetic engineering (Fig. 1). Our strategy to present LBTs on curli fibers allows high-density extracellular display of REE-specific binding moieties without the need for peptide purification or chemical conjugation (Table 1). The fibers aggregate into extended networks that could be purified away from the cells via a simple filtration set-up, allowing the bacteria to be reused for further material production without being tied up in metal binding. The curli-based filters are also more robust to

treatment conditions that might compromise the viability of cell-based sorbents or the structural integrity of other biopolymeric materials. The curli-LBT filters show selective REE binding in the presence of competing metals, with a preference for the heavier lanthanides, including Tb, Nd, Eu and Dy—some of the most critical REEs. Metal recovery was complete after a swift wash with dilute acid, allowing the filters to be reused multiple times with little loss of efficiency. This simple desorption step, which exploits the chemical resilience of amyloids compared to cells or other biopolymers, avoids the need for more expensive chelators. The filters can be dried for storage and are easier to handle than whole-cell sorbents.

LBT Variant	Amino Acid Sequence
LBT2	YIDTNNDGWIEGDELYIDTNNDGWIEGDELLA
LBT2*	YIGTNNGGWIGGGGLYIGTNNGGWIGGGGLLA
LBT4	YIDTNNDGWIEGDELYIDTNNDGWIEGDELYIDTNNDGWIEGDEL YIDTNNDGWIEGDELLA
LBT4*	YIGTNNGGWIGGGGLYIGTNNGGWIGGGGLYIGTNNGGWIGG GGLYIGTNNGGWIGGGGLLA
LBT6	YIDTNNDGWIEGDELYIDTNNDGWIEGDELYIDTNNDGWIEGDEL YIDTNNDGWIEGDELYIDTNNDGWIEGDELYIDTNNDGWIEGDE LLA
LBT6*	YIGTNNGGWIGGGGLYIGTNNGGWIGGGGLYIGTNNGGWIGG GGLYIGTNNGGWIGGGGLYIGTNNGGWIGGGGLYIGTNNGGWI GGGGLLA

Table 1. Peptide sequences for the lanthanide-binding tags (LBTs) used in the study.

Experimental

Cloning

Plasmids carrying CsgA-LBT variants were created by sub-cloning synthesized DNA fragments (Integrated DNA Technologies, USA) into a pET21d-PT7-csgACEG plasmid via Gibson Assembly. To create the negative control plasmid, the gene for maltose-binding protein (MBP) was subcloned from a pET21a-MBP-His plasmid (Addgene 38006) into pET21d in place of the csg genes. All plasmids were transformed into PQN4 cells (csg, λDE3).

Curli production

For curli fiber production, overnight cultures were expanded in LB supplemented with 10 μg/ml carbenicillin to an OD_{600} of 0.7, then 0.1 mM IPTG was added and protein expression was allowed to occur overnight at 30°C with shaking. Cultures were diluted 10× for OD_{600} measurement. To quantify curli production, 500 μl cultures were pelleted and resuspended in 15 μg/ml Congo Red for 5 min. The suspension was re-pelleted and the absorbance of the supernatant was read at 490 nm and used to determine the amount of Congo Red bound. Three sets of cultures were used for each expression study.

Curli immobilization

Filter-immobilization of curli fiber mats was performed as described previously,[35] with some modifications. Overnight cultures were vacuum-filtered through 5 μm polycarbonate membranes (Whatman® Nuclepore™, 47 mm diameter, Millipore, USA) to the point of saturation. The filters were treated with 8 M guanidinium chloride at room temperature for 15 min and washed 3× with deionized water. They were then exposed to 50 U/ml benzonase (with 2 μM $MgCl_2$) at 25°C for 1 hr, and filter-rinsed 3× with deionized water. The cleaned filters were air-dried at 50°C overnight and weighed to determine the mass of immobilized material.

SDS-PAGE

Filter-immobilized fibers were carefully scraped off membranes in a minimal volume of deionized water, resuspended in 500 μl hexafluoroisopropanol (HFIP), sonicated for 1 hr, and left to shake at room temperature for 5 hr. The HFIP was carefully evaporated under an airstream, and the dried material was resuspended in 6 M urea and sonicated to resuspend before being loaded for SDSPAGE (200 V, 30 min).

REE sorption

8 mm discs were punched from the filters for batch binding experiments. The filter discs were rinsed with and subsequently soaked in 0.2 M HEPES buffer (pH 7) for 1 hr prior to binding. Individual and mixed REE solutions were diluted from 1000 μg/ml stocks (High Purity Standards, USA) into HEPES buffer to the desired concentrations. Filters were exposed to REE solutions in 48-well plates with gentle shaking. Metal content of the supernatant was assayed using ICP-MS (Agilent Technologies, 7700x) with samples diluted in 2% HNO_3, using Indium as an internal standard. For end-point measurements, the metal solutions were removed after 30 min and the filters washed once with HEPES buffer; the wash was pooled with the metal solution for ICP-MS quantitation. Three filters were used for each sorption/desorption experiment. To test binding under various pH conditions, the pH of the HEPES buffer was adjusted accordingly and reconfirmed after metal dilution. Filter luminescence following Tb^{3+} sorption (200 μM) was imaged on a FluorChem M Imager under UV illumination with a 525 nm emission filter. Statistical analysis was performed using the Student's t-test with a 95% confidence interval.

Determination of binding affinity K_D

The binding affinity of individual lanthanides to curli-LBT4 filters was determined using a series of metal concentrations (50-250 μM). The amount of metal bound at each concentration was calculated and used to determine K_D in GraphPad Prism using global non-linear regression analysis of total and non-specific binding. Binding data from wild-type curli filters was used as the nonspecific contribution. Three sets of data were fitted for each metal.

REE desorption

8 mm filter discs were first exposed to 100 μM Tb^{3+} (or mixed Ln^{3+}) for 30 min to allow adsorption. The amount adsorbed

was determined as above. For desorption, filters were gently shaken with dilute HNO_3 at different pH at room temperature. The amount of Tb^{3+} recovered was determined from the supernatant using ICP-MS. The fraction or percentage of metal recovered was calculated relative to the amount of metal sorbed. For multiple sorption/desorption cycles, filters were rinsed 2× with deionized water and 2× with 0.2 M HEPES buffer (pH 7) following acid treatment, then soaked in the same buffer for 1 hr prior to metal exposure. Filters were air-dried at 50°C overnight and weighed both before the first cycle and at the end of the third cycle. Samples of the filter discs were also taken for SEM imaging.

REE sorption under flow

To study sorption under continuous flow, a 47 mm curli-LBT4 filter was enclosed in a filter holder (50 mm outer diameter, Membrane Solutions, USA). A 20 µM binary mixture of Ce^{3+} and Tb^{3+} (in 0.2 M HEPES, pH 7) was delivered to the filter holder in Teflon tubing using a peristaltic pump (MasterFlex, Cole-Parmer, USA) in single-pass at a flow rate of 0.2 ml/min. The entire apparatus (tubing and filter holder without filter) was first rinsed with 2% HNO_3, then the REE mixture to determine background metal sorption for normalization. At fixed time points, the outflow from the filter holder was sampled, and the metal concentration of each species, *C*, was quantified using ICP-MS. At the end of the run, the total outflow volume was measured and its metal composition quantified to calculate the total amount of each metal species adsorbed by the filters. Breakthrough was determined for C/C_0 = 0.05, where C_0 = 20 µM. Three separate runs were conducted using individual curli-LBT4 filters to ensure reproducibility of the observed binding trends.

Scanning electron microscopy

SEM images were obtained on a Zeiss Ultra Plus FE-SEM operated at 5 kV in SE2 mode. Air-dried filters were immobilized on aluminum stubs and sputter-coated with 5 nm gold for imaging.

Results and discussion

Expression and immobilization of curli fibers displaying LBTs

Chimeric CsgA proteins fused to LBTs of various lengths were expressed in PQN4, a previously engineered *E. coli* strain in which the entire curli operon was chromosomally deleted (Table 1). This strain does not produce any other exopolymers besides curli that might complicate analysis of lanthanide binding. Expression of 2×- and 4×- concatemeric LBT repeats compared favorably to wild-type CsgA (wt-CsgA), as determined by a pull-down assay using the amyloid-binding Congo Red dye, but a longer 6×-LBT variant gave lower curli production and a lower cell density at the end of expression, an indicator that the variant was toxic when over-expressed (ESI Fig. S1). Toxicity could be a consequence of the large size of the appended domain or the large number of negative charges introduced by acidic residues in LBT (five per repeat). Previous studies have shown that large domains exceeding 250 amino acids could be exported successfully through the curli biogenesis pathway, so long as the domain was largely unstructured or its folded structure did not exceed 2.5 nm in diameter.[48] Since the lanthanide-binding tag is unstructured in the absence of lanthanide ions,[41] it is unlikely that the size of larger concatamers was limiting expression. On the other hand, the additional charges on large LBT repeats could disrupt the electrostatic interaction between CsgA and CsgC, a periplasmic chaperone that prevents the intracellular aggregation of unsecreted CsgA.[49,50] Rampant periplasmic aggregation of CsgA could have led to cell lysis and limited overall curli production. When the LBT sequence was modified to switch all the acidic residues to glycine (LBT*), better expression was observed for 6×-LBT*, thus the highly-charged nature of high-repeat LBT variants was likely to have compromised curli production (Fig. S1). All three LBT variants formed large extracellular fiber meshes (Fig. S2) as observed previously with wt-CsgA expressed in the absence of CsgB and CsgF. Wt-CsgA, CsgA-LBT2 and CsgA-LBT4 variants were subsequently filter-immobilized on polycarbonate membranes for REE binding studies (~1 mg biomass per 47 mm filter).

Tb^{3+} abstraction using curli-LBT filters

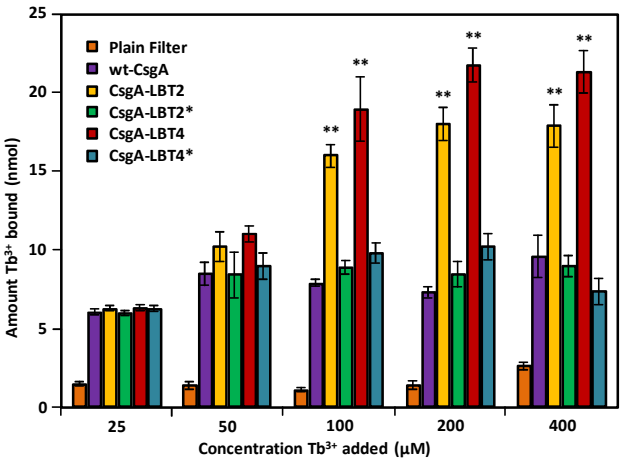

Figure 2. Tb^{3+} abstraction by curli-LBT filters, as determined by ICP-MS. Curli-LBT filters bound ~2.5× more Tb^{3+} than wt-CsgA filters at high Tb^{3+} concentrations. ** represents $p < 0.01$ (relative to wt-CsgA binding).

Batch sorption studies with the curli-LBT filters were first performed using Tb^{3+}, a critical rare earth metal and the canonical ligand for LBT. 8 mm filter discs were exposed to various concentrations of Tb^{3+}, and the quantity of metal adsorbed was determined by ICP-MS. The unmodified polycarbonate membranes bound a negligible amount of metal. Filters modified with curli-LBT bound ~2.5× more Tb^{3+} than wt-curli filters (Fig. 2), with LBT4 binding more Tb^{3+} than LBT2 (~43% vs. ~36% of 200 µM Tb^{3+}). LBT4 did not give double the binding capacity of LBT2, likely because some of the LBTs were occluded and not available for binding. Maximum binding was attained within 30 min (Fig. S3). CsgA contains

several acidic residues which could interact with metal ions, giving some baseline Tb^{3+} sorption. The addition of the LBTs increased overall binding but also added binding specificity for REEs via chelating residues. This is shown in Fig. 2, where modified filters lacking acidic residues in the LBT domains (LBT*) showed much diminished binding capacities for Tb^{3+}. Binding specificity is further evidenced by examining the luminescent properties of the filters. The LBT contains a tryptophan antenna residue that sensitizes the luminescence of bound lanthanide ions.[39] UV irradiation of Tb^{3+}-exposed filters showed distinctly higher luminescence for curli-LBT compared to wt-curli and curli-LBT* filters (Fig. 3), in correspondence with quantitative trends from ICP-MS.

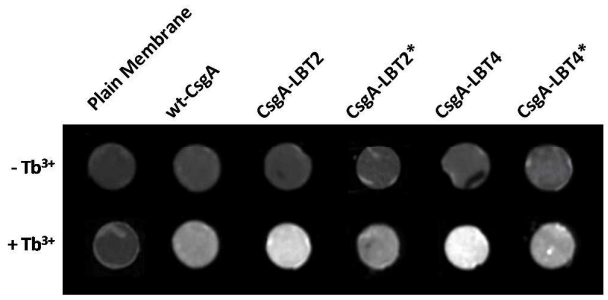

Figure 3. Optical image shows luminescence of filters with different types of modified curli fiber mats exposed to 100 µM Tb^{3+}. Consistent with quantitative binding studies, LBT2 and LBT4 filters gave the highest luminescence signals due to strong Tb^{3+}-LBT interactions. LBT2* and LBT4*, which did not contain chelating residues, gave only a low background signal comparable to wt-CsgA.

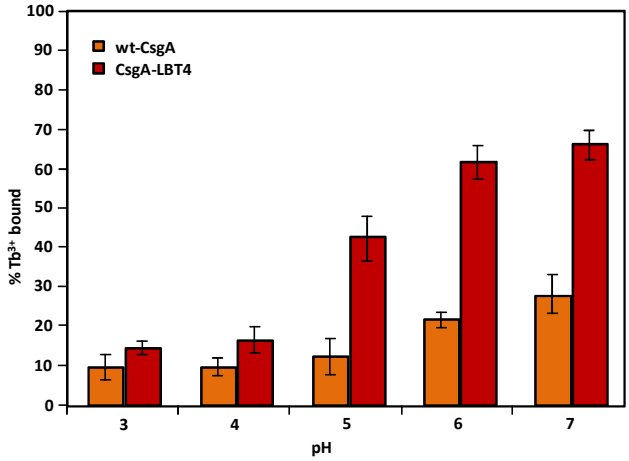

Figure 4. Binding of 100 µM Tb^{3+} by curli-LBT4 filters at different pH. Progressive protonation of the LBTs at low pH led to loss of Tb^{3+} binding. Optimal binding occurred at pH 6-7; below pH 4, the pK_a of the chelating carboxylate groups in LBTs, little binding was observed.

Sorption capacity peaked at 0.342 ± 0.022 mmol Tb^{3+} g^{-1} immobilized biomass for curli-LBT4 filters, which compared favorably to values of 0.01-1 mmol g^{-1} reported for cell-based biosorbents.[19,43,51] The calculated binding affinity for curli-LBT2 and curli-LBT4 were ~9.9 µM and 14.7 µM respectively. These values are much higher than the reported K_D for Tb^{3+} binding to purified LBT (~57 nM),[41] likely because not all the LBTs were exposed for binding following aggregation of curli fibers and immobilization of the fiber mats. Comparison of the sorption capacity of wt-CsgA (0.154 ± 0.014 mmol Tb^{3+} g^{-1}) and CsgA-LBT4 filters showed that 3.2 Tb^{3+} ions were bound per molecule of CsgA-LBT4. Because of its higher binding capacity, CsgA-LBT4 filters were used for all subsequent sorption experiments.

REE extraction typically involves acid leaching, thus Tb^{3+} sorption was measured in a range of acidic conditions (pH 3-7). Higher pH was not investigated as lanthanides formed insoluble hydroxides under basic conditions. Tb^{3+} binding by CsgA-LBT4 filters decreased rapidly at pH values below 5, and was comparable to wt-CsgA filters at pH 3 (Fig. 4). This was likely due to protonation of the chelating glutamate and aspartate residues, which have a pK_a around 3. The filters are thus most effective at pH 5-7.

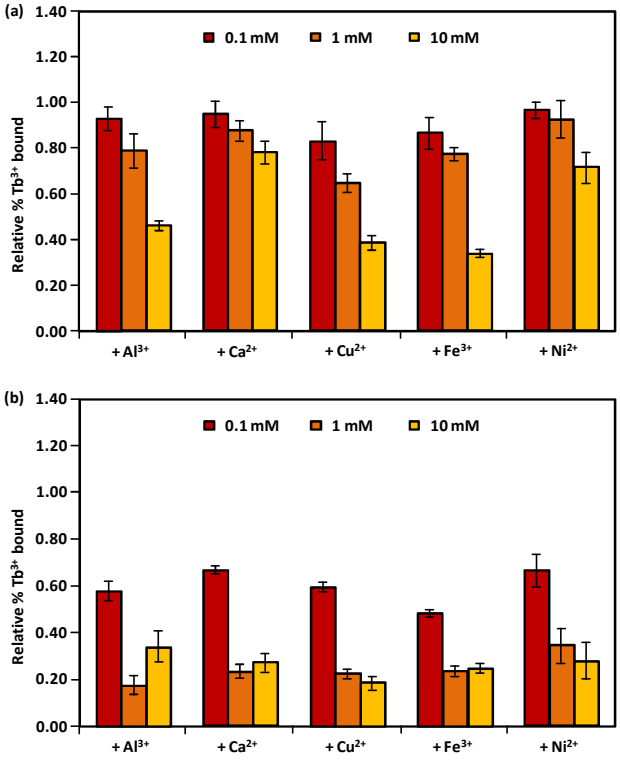

Figure 5. Binding of 100 µM Tb^{3+} by (a) CsgA-LBT4 and (b) wt-CsgA filters in the presence of other metals. Unlike the LBT4 filters, non-specific abstraction of Tb^{3+} to wt-CsgA filters was much reduced even at equimolar concentrations of competing metals.

Since REEs frequently coexist with other metals in ores and waste streams, we examined Tb^{3+} sorption by curli-LBT4 filters in the presence of other metal ions. Al^{3+}, Fe^{3+}, Ni^{2+} and Ca^{2+} did not significantly impact sorption of 100 µM Tb^{3+} at concentrations 10× higher, but Cu^{2+} reduced sorption by 50% (Fig. 5a). This inhibitory effect of copper was also reported for

the original LBT.[37] At concentrations 100× higher, Cu^{2+}, Al^{3+} and Fe^{3+} all led to much reduced Tb^{3+} binding. Overall, Tb^{3+} sorption to LBT4 filters was relatively unaffected by other metal ions except at much higher concentrations. This was unlike wt-CsgA filters, where equimolar quantities of other metals effectively outcompeted Tb^{3+} binding (Fig. 5b). This was further evidence of lanthanide specificity provided by the displayed LBTs.

Tb^{3+} recovery from curli-LBT filters

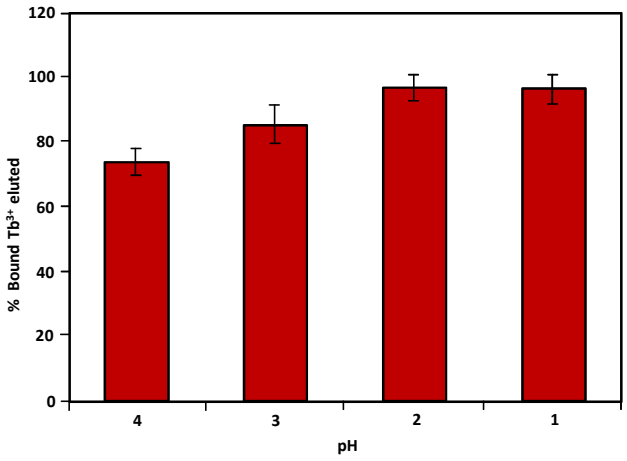

Figure 6. Desorption of Tb^{3+} from CsgA-LBT4 filters using different pH washes. Nitric acid at pH 2 (0.01 M) was sufficient to remove nearly all the bound Tb^{3+}.

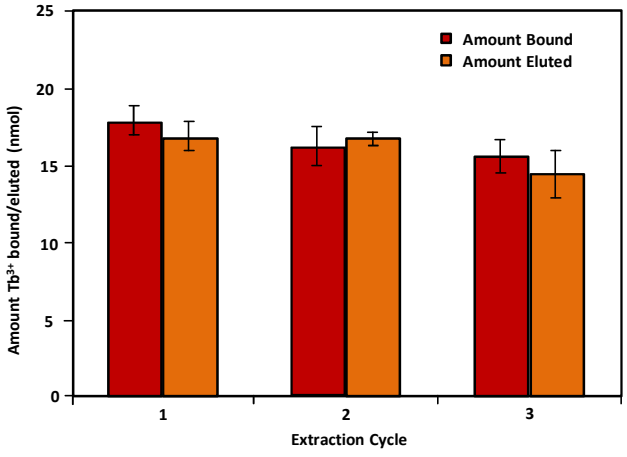

Figure 7. Curli-LBT4 filters can be used for multiple cycles of Tb^{3+} sorption/desorption with minimal loss of sorption capacity. 100 µM Tb^{3+} was used for sorption, and desorption was carried out with pH 2 nitric acid.

Desorption of sequestered Tb^{3+} from the filters was investigated using nitric acid, since low pH disrupts binding to LBT (Fig. 4). An initial pH screen (using different nitric acid concentrations) showed that complete recovery of bound Tb^{3+} was achieved at pH 2 (Fig. 6), and desorption was complete within 30 min (Fig. S4). Although organic ligands like citrate are also effective desorbents,[37,43] they are not specific for REEs, and much higher concentrations might be necessary if other metals are also bound to the filters, potentially increasing the cost of the process. We chose to simplify desorption using an acid wash, which could also facilitate the downstream REE sorting processes by not introducing additional ligands. The filters were subjected to multiple cycles of Tb^{3+} sorption/desorption, with a buffered wash following desorption to regenerate the chelating groups. There was no significant reduction in Tb^{3+} binding after three cycles (Fig. 7). Unlike with cell-based sorbents, where cell viability could be compromised by acid washes,[19] amyloids are more resilient to a variety of harsh environmental conditions. Curli fibers are able to fibrillate at low pH[52] and only disassemble on exposure to high concentrations of denaturants (e.g. formic acid, hexafluoroisopropanol). The dilute acid used for desorption here is unlikely to cause fiber disassembly, and indeed there was no detectable loss of mass from the filters, and the fiber mats were largely intact after three rounds of acid treatment (Fig. S5).

REE abstraction and recovery using curli-LBT filters

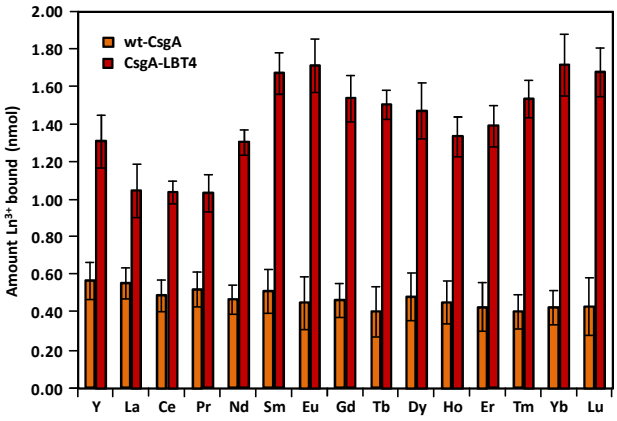

Figure 8. Adsorption of 100 µM mixed REEs to wt-CsgA and CsgA-LBT4 filters. The LBT4 filters showed a preference for binding heavier Ln^{3+}.

Table 2. Binding constants of curli-LBT4 filters for individual REEs, determined by exposing various concentrations of the Ln^{3+} to the filters.

REE	K_D (µM)
Tb^{3+}	14.7 ± 6.3
Eu^{3+}	10.9 ± 5.4
Dy^{3+}	15.1 ± 6.9
Nb^{3+}	51.5 ± 14.2
Y^{3+}	54.3 ± 20.7
Ce^{3+}	284 ± 36.5

We next investigated if CsgA-LBT4 filters could be used to abstract other REEs, using a mixed equimolar solution of 15 REEs (abbreviated Ln^{3+}). Although the lanthanides exhibit very similar physicochemical properties, there is a 20% contraction in ionic radii across the series, with a concomitant increase in Lewis acidity that favors binding of the heavier lanthanides to LBTs.[41] As shown in Fig. 8, curli-LBT4 filters bound the mid- to heavy lanthanides preferentially, as well as Y^{3+}, whose ionic radius is similar to that of the heavy REEs (HREEs). In contrast, no selectivity was observed for wt-CsgA filters. Calculated binding affinities for several of the REEs support the binding preference shown in Fig. 8, with Tb^{3+}, Eu^{3+} and Dy^{3+} being the strongest binders, followed by Nb^{3+} and Y^{3+}, and Ce^{3+} the weakest binders (Table 2). This suggests that CsgA-LBT filters could be used to selectively sequester most of the critical REEs, including Nb, Tb, Eu, Dy and Y. The bound Ln^{3+} could be recovered by washing with dilute nitric acid (Fig. 9).

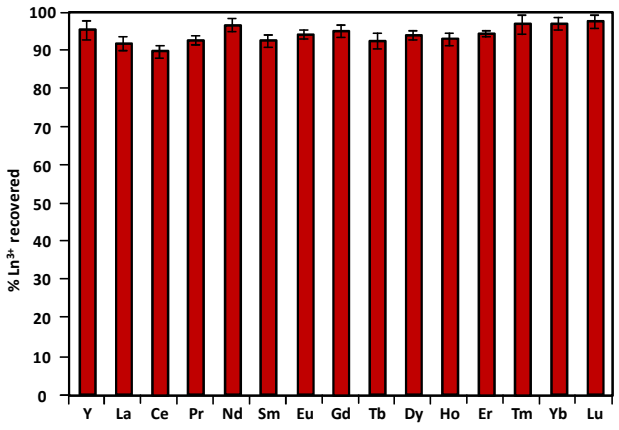

Figure 9. Bound Ln^{3+} could be desorbed from CsgA-LBT4 filters using pH 2 nitric acid.

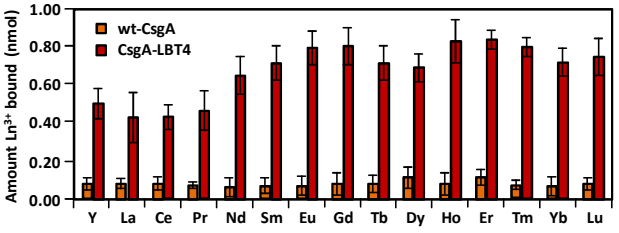

Figure 10. Adsorption of 100 µM mixed REEs by wt-CsgA and CsgA-LBT4 filters in the presence of mixed metals. Although overall sorption by the LBT filters decreased by ~50%, selectivity was retained relative to wt-CsgA filters.

We also examined REE adsorption from a metal mixture containing excess Al^{3+}, Ca^{2+}, Cu^{2+}, $Fe^{3+}$and Ni^{2+}, chosen to simulate waste streams from mine tailings and recycled end-of-life sources (Table S1).[2,53] Overall REE sorption by curli-LBT4 filters fell by ~50% in the presence of other metals, but selectivity for REEs improved over wt-CsgA filters, for which there was negligible REE adsorption (Fig. 10). The LBT filters also retained their selectivity for the HREEs (Fig. 10).

REE abstraction under flow conditions

CsgA-LBT4 filters could be adapted for separation under continuous flow, which is advantageous for REE recovery from more dilute streams. To investigate flow-based sorption, 20 µM of a binary Tb^{3+}-Ce^{3+} mixture was pumped through an encased filter without feed recycling. Breakthrough (measured at $C/C_0 = 0.05$) occurred earlier for Ce^{3+} (~47 min) compared to Tb^{3+} (~54 min), consistent with higher affinity of the LBTs for Tb^{3+} seen in batch sorption experiments (Fig. 11). There was competitive interaction between the two lanthanides, with stronger-binding Tb^{3+} ions displacing bound Ce^{3+} after the latter was saturated, leading to the observed overshoot ($C/C_0 > 1$) between 65-100 min. This was also confirmed by the different quantities of lanthanides adsorbed: 0.22 µmol Tb^{3+} compared to 0.14 µmol Ce^{3+}. Similar selectivity was not evident with wt-curli filters, where breakthrough for both lanthanides occurred at similar times, and the slopes of the breakthrough curves were more similar (Fig. 11).

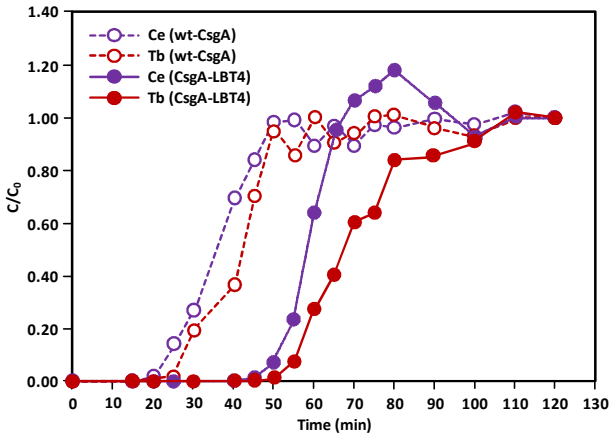

Figure 11. Breakthrough curves for Tb^{3+}-Ce^{3+} binary sorption to a CsgA-LBT4 filter under low-speed single-pass flow. C_0: 20 µM for each species; flow rate: 0.2 ml/min; biomass immobilized: 1.1 mg. Consistent with data from batch sorption, CsgA-LBT4 filters displayed a higher affinity for Tb^{3+} than Ce^{3+}, as shown by the longer time to breakthrough for Tb^{3+}, the gentler slope of the Tb^{3+} curve, and the overshoot seen with Ce^{3+}, an indication of Ce^{3+} displacement by Tb^{3+}. Data shown is representative of three separate runs using three different sets of filters.

Conclusions

Biofilms have long been utilized as passive sorption vessels to remove toxic species from wastewater, but as the focus of waste management turns towards resource recovery in addition to conventional remediation, there are potentially more lucrative niches which biofilm-based technologies can fill, provided they can be more selective in their binding targets. Here we have demonstrated one general approach to introducing greater selectivity, via the genetic modification of protein nanofibers in the extracellular matrix of biofilms to

display binding tags. Our approach complements existing approaches based on cell surface modification, but is advantageous because it treats the cells as foundries for the continued production of biosorbent, rather than as end-point sorbent products. Filters derived from the engineered fibers showed utility in the selective separation of REE from complex mixtures in both batch and continuous operations. The binding capacity of the CsgA-LBT4 filters was ~0.3 mmol Ln^{3+} g^{-1} immobilized biomass when used for batch sorption of pure lanthanides. This value is similar to that reported for *P. aeruginosa* and a range of other bacteria and algae (0.01-1 mmol g^{-1}),[19,51] and better than *Caulobacter crescentus* with surface-displayed LBTs reported by Park *et al* (~0.06 mmol g^{-1}).[43] The curli-LBT filters are best suited for sorption at REE concentrations above 50 µM (>1 ppm) and such concentrations are often found in bauxite residue (red mud), phosphogypsum, and metallurgical slag derived from recycling waste electric and electronic equipment. Further optimization of our bench-scale experiments could potentially increase separation efficiency and provide greater resolution for the recovery of the different lanthanides. Overall, our results establish the potential of engineered biofilm-derived materials as biotechnological tools for selective separations processes.

Conflicts of interest

There are no conflicts to declare.

Acknowledgements

This work was funded by NSF Grant 1410751 (Division of Materials Research) and the Wyss Institute for Biologically Inspired Engineering. It made use of the shared facilities at the Harvard Center for Nanoscale Systems at Harvard University. A. M.-B. acknowledges Frontier Research Fellowship. P. K. T. acknowledges support by A*STAR in Singapore.

References

1 E. Alonso, A. M. Sherman, T. J. Wallington, M. P. Everson, F. R. Field, R. Roth and R. E. Kirchain, *Environ. Sci. Technol.*, 2012, **46**, 3406-3414.
2 H. M. D. Bandara, K. D. Field and M. H. Emmert, *Green Chem.*, 2016, **18**, 753-759.
3 J. H. Rademaker, R. Kleijn and Y. Yang, *Environ. Sci. Technol.*, 2013, **47**, 10129-10136.
4 J. R. Dodson, H. L. Parker, A. Munoz Garcia, A. Hicken, K. Asemave, T. J. Farmer, H. He, J. H. Clark and A. J. Hunt, *Green Chem.*, 2015, **17**, 1951-1965.
5 D. Puyol, D. J. Batstone, T. Hülsen, S. Astals, M. Peces and J. O. Krömer, *Front. Microbiol.*, 2016, **7**, 2106.
6 C. B. McLellan, D. G. Corder and H. S. Ali, *Minerals*, 2013, **3**,304-317.
7 F. Xie, T. A. Zhang, D. Dreisinger and F. Doyle, *Miner. Eng.*, 2014, **56**, 10-28.
8 M. K. Jha, A. Kumari, R. Panda, J. Rajesh Kumar, K. Yoo and J. Y. Lee, *Hydrometallurgy*, 2016, **165**, 2-26.
9 K. Binnemans, P. T. Jones, B. Blanpain, T. Van Gerven, Y. Yang, A. Walton and M. Buchert, *J. Clean. Prod.*, 2013, **51**, 1-22.
10 D. Kim, L. E. Powell, L. H. Delmau, E. S. Peterson, J. Herchenroeder and R. R. Bhave, *Environ. Sci. Technol.*, 2015, **49**, 9452-9459.
11 G. M. Gadd, *Microbiology*, 2010, **156**, 609-643.
12 P. K. R. Tay, P. Q. Nguyen and N. S. Joshi, *ACS Synth. Biol.*, 2017, **6**, 1841-1850.
13 A. Pol, T. R. M. Barends, A. Dietl, A. F. Khadem, J. Eygensteyn, M. S. M. Jetten and H. J. M. Op den Camp, *Environ. Microbiol.*, 2014, **16**, 255-264.
14 E. Skovran and N. C. Martinez-Gomez, *Science*, 2015, **348**, 862-863.
15 M. Wehrmann, P. Billard, A. Martin-Meriadec, A. Zegeye and J. Klebensberger, *mBio*, 2017, **8**, e00570-17.
16 Y. Andres, A. C. Texier and P. Le Cloirec, *Environ. Technol.*, 2003, **24**, 1367-1375.
17 H. Moriwaki and H. Yamamoto, *Appl. Microbiol. Biotechnol.*, 2013, **97**, 1-8.
18 H. Moriwaki, R. Masuda, Y. Yamazaki, K. Horiuchi, M. Miyashita, J. Kasahara, T. Tanaka and H. Yamamoto, *ACS Appl. Mater. Interfaces*, 2016, **8**, 26524-26531.
19 L. Philip, L. Iyengar and C. Venkobachar, *J. Ind. Microbiol. Biotechnol.*, 2000, **25**, 1-7.
20 A. C. Texier, Y. Andres and P. L. Cloirec, *Environ. Technol.*, 1997, **18**, 835-841.
21 W. D. Bonificio, and D. R. Clarke, *Environ. Sci. Technol. Lett.*, 2016, **3**, 180-184.
22 A. C. Texier, Y. Andres, and P. Le Cloirec, *Wat. Sci. Technol.*, 2000, **42**, 91-94.
23 H. R. Dash and S. Das, *RSC Adv.*, 2016, **6**, 109793-109802.
24 A. Upadhyay, M. Kochar, M. V. Rajam and S. Srivastava, *Front. Microbiol.*, 2017, **8**, 284.
25 F. Wang, J. Zhao, F. Pan, H. Zhou, X. Yang, W. Li, and H. Liu, *Ind. Eng. Chem. Res.*, 2013, **52**, 3453-3461.
26 S. Wang, M. F. Hamza, T. Vincent, C. Faur and E. Guibal, *J. Colloid Interface Sci.*, 2017, **504**, 780-789.
27 F. Wang, J. Zhao, X. Wei, F. Huo, W. Li, Q. Hu and H. Liu, *J. Chem. Technol. Biotechnol.*, 2014, **89**, 969-977.
28 P. Q. Nguyen, N.-M. Dorval Courchesne, A., Duraj-Thatte, P. Praveschotinunt and N. S. Joshi, *Adv. Mat.*, **2018**, doi 10.1002/adma.201704847
29 A. Y. Chen, Z. Deng, A. N. Billings, U. O. S. Seker, M. Y. Lu, R. J. Citorik, B. Zakeri, and T. K. Lu, *Nat. Mater.*, 2014, **13**, 515-523.
30 P. Q. Nguyen, Z. Botyanszki, P. K. R. Tay and N. S. Joshi, *Nat. Commun.*, 2014, **5**, 4945.
31 C. Zhong, T. Gurry, A. A. Cheng, J. Downey, Z. Deng, C. M. Stultz and T. K. Lu, *Nat. Nanotechnol.*, 2014, **9**, 858-866.
32 Z. Botyanszki, P. K. R. Tay, P. Q. Nguyen, M. G. Nussbaumer and N. S. Joshi, *Biotechnol. Bioeng.*, 2015, **112**, 2016-2024.
33 M. G. Nussbaumer, P. Q. Nguyen, P. K. R. Tay, A. Naydich, E. Hysi, Z. Botyanszki and N. S. Joshi, *ChemCatChem*, 2017, **9**, 4328-4333.
34 U. O. S. Seker, A. Y. Chen, R. J. Citorik and T. K. Lu, *ACS Synth. Biol.*, 2017, **6**, 266-275.
35 N.-M. Dorval Courchesne, A. Duraj-Thatte, P. K. R. Tay, P. Q. Nguyen and N. S. Joshi, ACS *Biomater. Sci. Eng.*, 2017, **3**, 733-741.
36 K. Barthelmes, A. M. Reynolds, E. Peisach, H. R. A. Jonker, N. J. DeNunzio, K. N. Allen, B. Imperiali and H. Schwalbe, *J. Amer. Chem. Soc.*, 2011, **133**, 808-819.
37 K. J. Franz, M. Nitz and B. Imperiali, *Chembiochem*, 2003, **4**, 265-271.
38 L. J. Martin, M. J. Hahnke, M. Nitz, J. Wohnert, N. R. Silvaggi, K. N. Allen, H. Schwalbe and B. Imperiali, *J. Amer. Chem. Soc.*, 2007, **129**, 7106-7113.
39 B. R. Sculimbrene and B. Imperiali, *J. Amer. Chem. Soc.*, 2006, **128**, 7346-7352.

40 N. R. Silvaggi, L. J. Martin, H. Schwalbe, B. Imperiali and K. N. Allen, *J. Amer. Chem. Soc.*, 2007, **129**, 7114-7120.
41 M. Nitz, M. Sherawat, K. J. Franz, E. Peisach, K. N. Allen and B. Imperiali, *Angew. Chem. Int. Ed.*, 2004, **43**, 3682-3685.
42 H. Liang, X. Deng, M. Bosscher, Q. Ji, M. P. Jensen and C. He, *J. Amer. Chem. Soc.*, 2013, **135**, 2037-2039.
43 D. M. Park, D. W. Reed, M. C. Yung, A. Eslamimanesh, M. M. Lencka, A. Anderko, Y. Fujita, R. E. Riman, A. Navrotsky and Y. Jiao, *Environ. Sci. Technol.*, 2016, **50**, 2735-2742.
44 S. Bolisetty and R. Mezzenga, *Nat. Nanotechnol.*, 2016, **11**, 365-371.
45 C. W. am Ende, H. Y. Meng, M. Ye, A. K. Pandey and N. J. Zondlo, *ChemBioChem*, 2010, **11**, 1738-1747.
46 E. Pidcock and G. R. Moore, *J. Biol. Inorg. Chem.*, 2001, **6**, 479-489.
47 L. Shunyi, Y. Wei, M. W. Anna, Jr. B. Doyle, T. Harianto, Z. Huan-Xiang and Y. J. Jenny, *FEBS J*, 2008, **275**, 5048-5061.
48 N. Van Gerven, P. Goyal, G. Vandenbussche, M. De Kerpel, W. Jonckheere, H. De Greve and H. Remaut, *Mol. Microbiol.*, 2014, **91**, 1022-1035.
49 M. L. Evans, E. Chorell, J. D. Taylor, J. Aden, A. Gotheson, F. Li, M. Koch, L. Sefer, S. J. Matthews, P. Wittung-Stafshede, F. Almqvist and M. R. Chapman, *Mol. Cell*, 2015, **57**, 445-455.
50 J. D. Taylor, W. J. Hawthorne, J. Lo, A. Dear, N. Jain, G. Meisl, M. Andreasen, C. Fletcher, M. Koch, N. Darvill, N. Scull, A. Escalera-Maurer, L. Sefer, R. Wenman, S. Lambert, J. Jean, Y. Xu, B. Turner, S. G. Kazarian, M. R. Chapman, D. Bubeck, A. de Simone, T. P. Knowles and S. J. Matthews, *Sci. Rep.*, 2016, **6**, 24656.
51 T. Tsuruta, *Journal of Rare Earths*, 2007, **25**, 526-532.
52 M. S. Dueholm, S. B. Nielsen, K. L. Hein, P. Nissen, M. Chapman, G. Christiansen, P. H. Nielsen and D. E. Otzen, *Biochemistry*, 2011, **50**, 8281-8290.
53 C. Ayora, F. Macías, E. Torres, A. Lozano, S. Carrero, J.-M. Nieto, R. Pérez-Lopez, A. Fernández-Martínez and H. Castillo-Michel, *Environ. Sci. Technol.*, 2016, **50**, 8255-8262.